

Estimation of Leaf Area Index Over Heterogeneous Regions Using the Vegetation Type Information and PROSAIL Model

Yangyang Zhang¹, Xu Han, and Jian Yang²

Abstract—The leaf area index (LAI) is a parameter that can indicate the vegetation canopy structure and accurately reflect the growth state of vegetation. Most studies estimate the LAI of single vegetation in homogeneous areas, but only few studies have explored the LAI inversion of heterogeneous areas. Canopy heterogeneity in heterogeneous regions may increase the uncertainty and difficulty of LAI quantitative inversion. Therefore, LAI retrieval in heterogeneous areas needs to be studied to obtain LAI distribution maps in a large spatial range. In this study, an LAI inversion model considering vegetation types was proposed based on the look-up table (LUT) method and the PROSAIL model for estimating the LAI of heterogeneous surfaces. First, the LUTs of different vegetation types were generated by using PROSAIL with a priori information of multispecies. Second, the corresponding LUT for LAI estimation was selected according to the determined vegetation types. Finally, a parametric sensitivity analysis was conducted based on the PROSAIL model to recognize the key parameters of the algorithm's efficiency. Results show that the approach considering vegetation types ($R^2 = 0.63$, RMSE = 0.75 / $R^2 = 0.64$, RMSE = 0.50) is superior to the traditional approach that does not consider vegetation types ($R^2 = 0.50$, RMSE = 1.32 / $R^2 = 0.17$, RMSE = 1.81). Therefore, the former approach can greatly improve the accuracy of multispecies LAI estimation, especially for areas with high canopy heterogeneity. The proposed approach for multispecies vegetation LAI retrieval can provide new insights for studying the ecological status of complex land surface regions and exhibit an excellent potential for the extended application of the PROSAIL model in heterogeneous areas.

Index Terms—Heterogeneous areas, leaf area index (LAI), look-up table (LUT), prosail, vegetation types.

I. INTRODUCTION

LEAF area index (LAI), as an essential structural parameter of the ecosystem, can accurately reflect the physiological state of vegetation [1]. LAI is a key indicator that considerably affects the energy and material exchange processes in the canopy

atmosphere, such as vegetation photosynthesis, respiration, and transpiration, and is an indispensable parameter in most hydrological, ecological, biogeochemical, and climate models [1], [2], [3]. Hence, accurate LAI retrieval is an inevitable step in monitoring vegetation growth, precision agriculture, yield prediction, and biomass estimation [4]. For LAI estimation, empirical models are constructed using remote sensing reflectance or its corresponding mathematical form as the natural quantity and LAI as the dependent variable [5]. These models are relatively simple and fast and usually obtain good regressions. However, statistical models lack physical mechanism and generality, which make them only suitable for specific areas [4]. By contrast, the radiative transfer model (RTM), which is a model of canopy, leaf, and soil properties, describes the relationship between solar radiation and vegetation [6]. Thus, vegetation physicochemical parameters and canopy spectral reflectance are linked by RTM [7]. PROSAIL, a widely used canopy physical model [8], is a coupling of the PROSPECT [9] and SAIL models [10]. The PROSPECT model is a leaf optical model developed by Jacquemoud and Baret [9]. Several versions of this model have also been developed through multiple updates [11], [12], [13]. The PROSPECT model assumes a functional relationship between leaf reflectance and transmittance and biophysical and biochemical parameters, and uses this functional relationship to simulate leaf reflectance and transmittance in the range of 400–2500 nm [14]. SAIL is one of the earliest canopy RTMs [10], [15], and is an extension of the one-dimensional model developed by Suits [16]. This model simulates the duality reflection factor of vegetation canopy composed of mixed media by solving four upward/downward scattering and absorbing radiation fluxes. The SAIL model requires input of leaf transmittance and reflectance to simulate canopy reflectance. Given that these two parameters can be simulated by the PROSPECT model, both PROSPECT and SAIL are coupled to obtain the PROSAIL model. In this model, the leaf reflectance and transmittance output from the PROSPECT model are used as input of the SAIL model to simulate the canopy reflection in the range of 400–2500 nm. The PROSAIL model has several versions with many improvements, and has been validated by many studies [17], [18]. In the forward mode, the reflectance of a vegetation canopy can be obtained by inputting different parameters based on the PROSAIL model. Meanwhile, in the inverse mode, the biochemical parameters of vegetation are retrieved based on

Manuscript received 22 March 2023; revised 25 April 2023 and 23 May 2023; accepted 24 May 2023. Date of publication 7 June 2023; date of current version 21 June 2023. This work was supported in part by the Knowledge Innovation Program of Wuhan-Shuguang Project under Grant 2022010801020433, in part by the National Natural Science Foundation of China (NSFC) under Grant 42271388 and Grant 41801268, and in part by the Special Fund of Hubei LuoJia Laboratory under Grant 220100034. (Corresponding author: Jian Yang.)

Yangyang Zhang and Xu Han are with the Wuhan City Polytechnic, Wuhan 430074, China (e-mail: zhangyangyang@cug.edu.cn; whanx@cug.edu.cn).

Jian Yang is with the China University of Geoscience, Wuhan 430074, China (e-mail: yangjian@cug.edu.cn).

Digital Object Identifier 10.1109/JSTARS.2023.3283535

spectral data and by using PROSAIL. Thus, previous studies have widely used PROSAIL to retrieve the LAI of various vegetation types, such as wheat [19], [20], [21], [22], maize [23], [24], and sugar beet [25], [26]. While these studies mainly focused on the LAI retrieval of single vegetation type in homogeneous areas, the LAI estimation of multispecies vegetation in heterogeneous areas attracted limited attention [27] mainly because the underlying physical assumption of the PROSAIL model is that the scattering surface is uniform. Thus, PROSAIL was suggested to be applied in homogeneous vegetation canopies [28], [29], [30]. The PROSAIL model is designed to limit the number of possible variable parameters. Although not very realistic, doing so allows for short computation times and easier inversions. By contrast, 3-D RTMs provide a detailed description of canopy layers and components through a number of variables that can be fixed using a priori knowledge or retained as variable parameters [31]. Hence, compared with complex 3-D RTMs, the PROSAIL model needs fewer input parameters, has easier acquisition, and is computationally less intensive [32]. The application of this model needs to be extended to heterogeneous surface regions that contain multiple species of vegetation. Natural environments are often heterogeneous, and they typically contain multiple species of vegetation. However, differences in background reflectance, canopy closure, stand age, and other aspects in heterogeneous regions will aggravate the degree of canopy heterogeneity, thus increasing the uncertainty of LAI quantitative inversion. In this case, surface heterogeneity needs to be properly expressed, its influence on the LAI inversion model should be weakened, and the accuracy of LAI estimation of heterogeneous surfaces must be improved.

Using the PROSAIL model for LAI inversion typically follows three strategies, namely, iterative optimization [33], [34], look-up table (LUT) [24], [35], [36], and hybrid inversion [30], [37], [38], [39]. The iterative optimization method is computationally intensive, has poor convergence, and the accuracy of its LAI estimation depends on the preliminary values of model parameters. LUT estimates LAI through a multisolution database, hence, largely avoiding the effects of measured and model errors [40], thus improving the accuracy and robustness of the LAI estimation [41]. Therefore, LUT is a universal and simple method for LAI estimation. Although the hybrid inversion method is efficient, its procedures are not sufficiently clear and transparent [22]. Several studies have also shown that LUT exhibits a better LAI estimation performance than other strategies based on PROSAIL [3], [4], [20], [42]. Due to its stability and general robustness, LUT is widely used for LAI estimation [20], [22], [42].

Remote sensing can monitor a wide range, and the high heterogeneity of vegetation in the region will increase the difficulty of LAI inversion. The traditional LUT method does not consider the heterogeneity of vegetation types [25]. All vegetation types generate a unique LUT based on the PROSAIL model according to a uniform input parameter distribution and range, which are used for the LAI inversion of heterogeneous vegetation types. Aiming at the uncertainty of LAI inversion in heterogeneous areas, an LAI inversion model considering vegetation types was constructed based on the LUT method and the PROSAIL

model. Unlike the traditional method, the proposed method considers the heterogeneity of vegetation types. Different prior distributions of parameters related to heterogeneous vegetation were obtained and used as constraints to generate different LUTs for specific vegetation and the overall LUT. The addition of prior knowledge can address the problem in physical model inversion, and considering vegetation types can reduce the complexity of heterogeneous areas, thereby facilitating the LAI inversion of large spatial scale and complex areas. The main purposes of this study are 1) to evaluate the applicability of the LAI inversion model considering vegetation types in heterogeneous areas; and 2) to discuss the effect of different input parameters of the PROSAIL model on LAI estimation based on a sensitivity analysis in heterogeneous regions.

II. STUDY AREA AND DATA

A. Study Area

Measured data were collected in two study areas with different vegetation cover and species. The first study area was located around the village of Neusling in Germany, which contains representative samples of a wide range of important crops. The climate of the region is humid all year round, with temperature and rainfall averaging 7.4 °C and 750–850 mm, respectively. Various crop types are distributed in the study area, including winter wheat, winter barely, potato, corn, and rapeseed, and each crop type has different canopy structure characteristics, thus ensuring the heterogeneity of the study area. Fig. 1(a) presents results of an airborne flight over the study area on April 28, 2012.

The second study area was located in the downstream area of the Heihe River Basin in China, which is one of the three major inland rivers in China that originates from the Qilian Mountains and is situated in the middle of the Hexi Corridor with an altitude range of 875–5519 m. The basin is in the northwest arid zone and has a typical continental arid climate, sparse and concentrated precipitation, abundant sunshine, and temperature that varies widely from day to night. The annual rainfall in the downstream area of the Heihe River Basin is only 47 mm, and the average annual temperature is about 8 °C to 10 °C. Environmental changes, such as grassland degradation, soil erosion, and species loss, have a significant impact on the ecosystem of the Hexi Corridor, and the Heihe River Basin is critical to maintaining the ecological balance of this Corridor.

Various vegetation types, including shrub, meadow, cultivated vegetation, and sparse desert vegetation, are distributed in the Heihe River Basin, and its downstream area shows the highest level of ecological deterioration [43]. Therefore, the downstream area was selected as the second study area for LAI estimation to provide a reference for the ecological evaluation of the downstream area [see Fig. 2(b)].

Different types of vegetation lead to differences in appearance and canopy structure, which in turn aggravates the degree of regional heterogeneity and affects the inversion accuracy of LAI on heterogeneous surfaces. Moreover, the canopy structure characteristics of cultivated crops and natural vegetation are different, and the selection of the two study areas ensures a surface difference, hence highlighting the usability of this study.

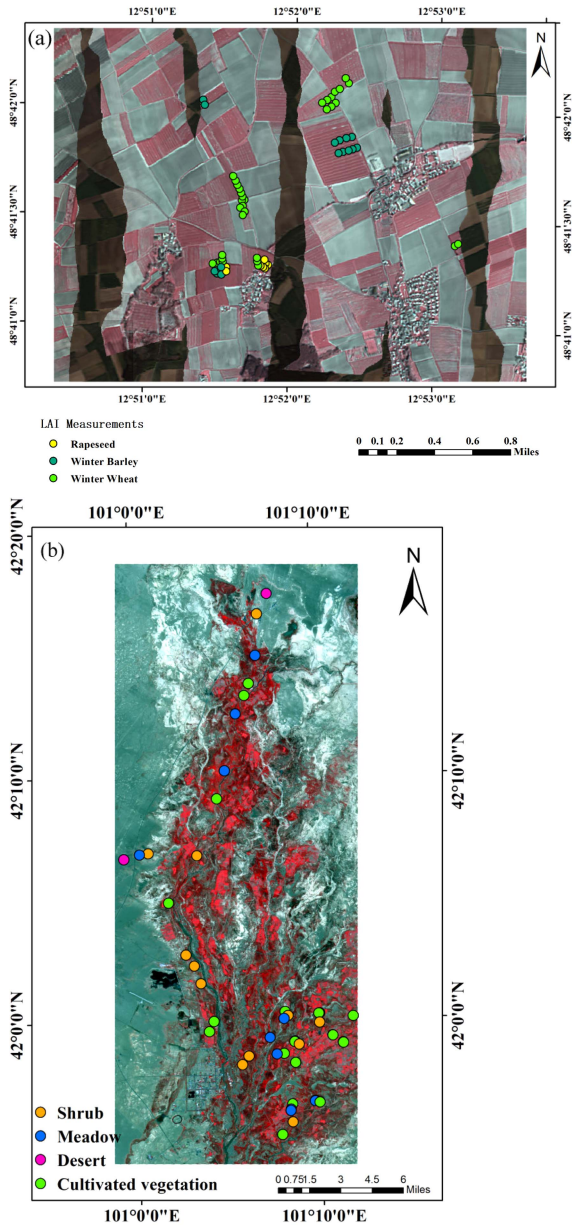


Fig. 1. (a) Study area in the village of Neusling in Germany. The LAI measurement points and remote sensing data were taken from an airborne image acquired on April 28, 2012 [the coverage of the SWIR data (colored infrared) is layered on top of the VIS and NIR extent (true color)]. (b) Study area in the downstream area of the Heihe River Basin in China. The LAI measurement points and remote sensing data were taken from a Chinese High-Resolution Satellite 1 (GF-1) image with false color composite taken on July 29, 2014 (R = near infrared, G = red, B = green).

B. Field Measurement Data

The Li-COR LAI-2200 plant canopy analyzer, which is the most widely utilized nondestructive LAI measurement instrument in agriculture, was used collect LAI in the two study areas. Based on hemispherical photography, the device determines LAI using this inversion of the gap fraction and estimates the probability of a ray of light to pass through a canopy having no contact with the plant material, thus quantifying the fraction of visible (VIS) sky. To ensure the accuracy of LAI measurements,

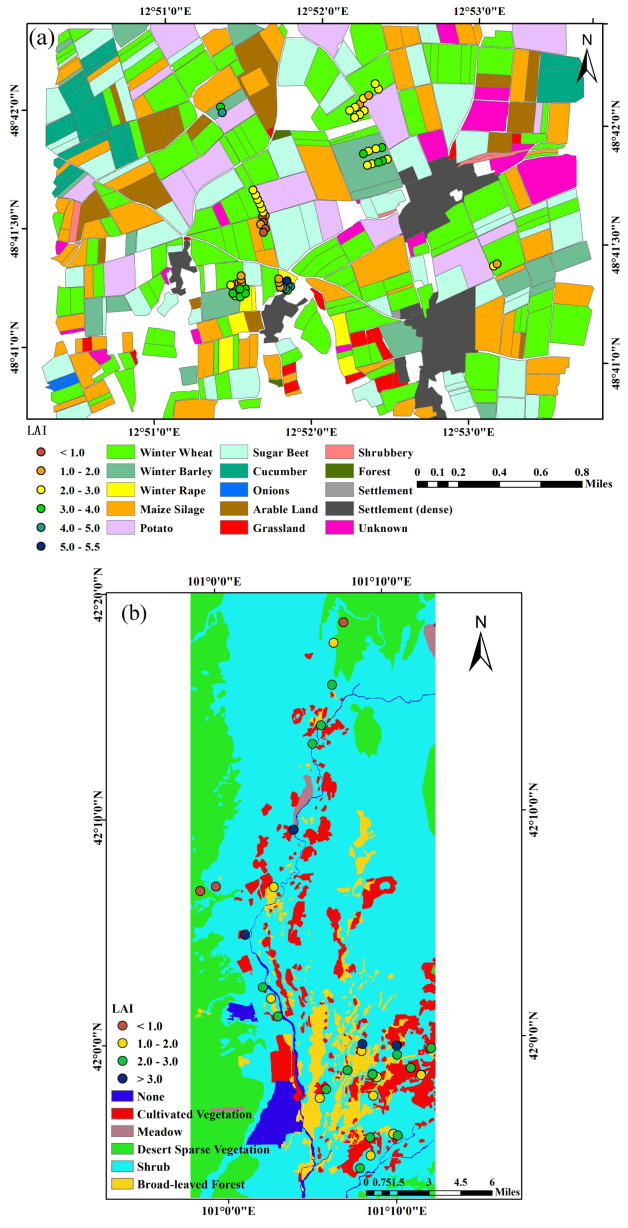


Fig. 2. Land cover map of the two study areas based on field observations and locations of all LAI measured points, expressed as collected LAI values. (a) Neusling study area. (b) Heihe River Basin study area.

each sample was repeatedly measured two times, and their mean values were taken as the final value. During the field measurements, all available standards of measurement conditions were followed, such as using a 180° view cap to prevent falsified measurements by the operator, avoiding direct sunlight, and maintaining the uniform azimuthal orientation of the device throughout the repetitions.

The LAI sampling points in the Neusling study area were acquired on April 28, 2012, and their distribution locations are shown in Fig. 1(a). The sample points were selected to be representative and to show the potential heterogeneity of the field. A minimum distance of 20 m was maintained between each sampling point to prevent recording redundant and repetitive information. Field measurements of typical crop LAI were

conducted in parallel with an airborne flight on the study area. A total of 61 field measurement samples were collected from different vegetation types, including winter wheat, winter barley, and rapeseed, after elimination the anomalous measured values. Winter wheat had 33 sample plots, the winter barley had 17 sample plots, and rapeseed had 11 sample plots. The Li-COR LAI-2200 plant canopy analyzer was used to observe the crop canopy LAI. The sampling strategy was to randomly distribute eight replicate canopies and two reference measurements per field measurement site.

Field measurements of vegetation LAI on the downstream surface of the Heihe River Basin were conducted from July 22 to August 1, 2014. Based on the distribution characteristics of the vegetation in the study area, the vegetation region with a uniform area distribution of greater than $100\text{ m} \times 100\text{ m}$ was used as the measurement site. A total of 34 field measurement samples were collected from different vegetation types, including shrub, cultivated vegetation, and meadow, after eliminating the anomalous measured values. The Li-COR LAI-2200 plant canopy analyzer was also used to observe the vegetation canopy LAI. The mean measured LAI for each sample site was obtained from the incident radiation from one above-canopy and four below-canopy measurements, and the measurement was repeated twice for each sample site [44]. Considering the specific categories of vegetation, the LAI measurements were classified into the three main categories of meadow, shrub, and cultivated vegetation. The meadow category consisted of five sample plots, including bitter bean, Asteraceae, weed, and reed, the shrub category had 12 sample plots, including different types of tamarisk, and cultivated vegetation had 15 sample plots. The remaining LAI field measurements also included two desert sparse vegetation sample sites.

By measuring the parameters of different vegetation types, this study analyzed the possibility of using the PROSAIL model to estimate LAI in multispecies vegetation with canopy heterogeneity. All field LAI measurements for the two study sites were downloaded from EnMAP [45] and the National Tibetan Plateau Data Center (<http://data.tpdc.ac.cn>), respectively.

C. Remote Sensing Data

To evaluate the performance of the LUT approach for multispecies vegetation LAI estimation, airborne, and satellite data were selected for each of the two study areas. The airborne data for the first study area (Neusling) was obtained by using the Airborne Imaging Spectrometer Airborne Visible and Near Infrared Spectrometer (AVIS-3) on April 28, 2012. Based on the first- and second-generation AVIS, the third generation AVIS-3 has been under development since 2006 with a higher spectral resolution and the ability to measure spectra in the short-wavelength infrared (SWIR) spectral range. The spectral region of the VNIR detector ranges between 400 and 1000 nm, and the newly added SWIR spectrometer has a sensitivity of 900–1750 nm. A series of preprocessing operations were performed on the AVIS-3 airborne data, including sensor calibration to remove systemic noise and deficiencies from the data, geometric correction to equalize aircraft motions during recording,

and ortho-rectification and radiometric calibration to convert the nondimensional grey values to radiance and reflectance. The maximal signal-to-noise ratio was 65 dB (1743:1). After all correction steps, the spectral range of AVIS-3 data was 477–1704 nm in 197 spectral bands, of which the spectral resolution in the 477–994 nm region was 5.8 nm, while that in the 994–1704 nm region was 6.6 nm. The spatial resolution of the AVIS-3 data was 4 m.

During preprocessing, the six overlapping original flight plans covering the study area were not sufficient to guarantee a complete coverage of the SWIR sensor, thus resulting in image gaps in the SWIR spectral range, as shown in Fig. 1. However, estimation the LAI of multivegetation is the focus of this study, and the selected measured points are outside the strip gaps. Therefore, the gaps of the SWIR sensor do not affect the final evaluation of the results. The AVIS-3 airborne data covering the study area were also downloaded from EnMAP [45].

The satellite data for the second study area (Heihe River Basin) were obtained from Chinese High-Resolution Satellite 1 (GF-1) images taken on July 29, 2014. The GF-1 data contained four multispectral bands, namely, blue (450–520 nm), green (520–590 nm), red (630–690 nm), and near-infrared (770–890 nm) and the spatial resolution of the GF-1 data was 16 m. The ENVI 5.3 software required for the quantitative inversion of remote sensing data was used to preprocess GF-1 data. The main processes involved included radiometric correction, atmospheric correction, and geometric correction [46]. Radiometric correction removed the influence of the sensor itself and converted the digital number values into apparent radiance, which is an important step in producing high-quality remote sensing data. Atmospheric correction was performed to obtain the reflectance by eliminating the radiometric errors caused by atmospheric influences. Geometric correction removed or corrected the geometric errors in the remote sensing image. The AVIS-3 and GF-1 data were preprocessed to convert image gray values into reflectance for quantitative inversion.

D. Land Cover Map

The Neusling study area had diverse crop types, including winter wheat, winter barley, maize, and rapeseed. As the key input data for the proposed LAI inversion model, land cover map data were used to determine the specific vegetation type for each pixel in the airborne image. The land cover mapping of the entire Neusling test site was carried out in May 2012, and the land cover map of the study area is shown in Fig. 2(a). The land cover map was resampled to 4 m using the nearest-neighbor method to maintain consistency with the spatial resolution of airborne data. The land cover map covering the study area was also downloaded from EnMAP [45].

The Heihe River Basin study area had diverse vegetation types, including sparse desert vegetation, shrub, cultivated vegetation, meadow, and extensive Gobi [43]. The 1:100000 vegetation map of the Heihe River Basin was obtained from the National Tibetan Plateau Data Center [47] and was resampled to 16 m for consistency with the spatial resolution of the GF-1 satellite data shown in Fig. 2(b).

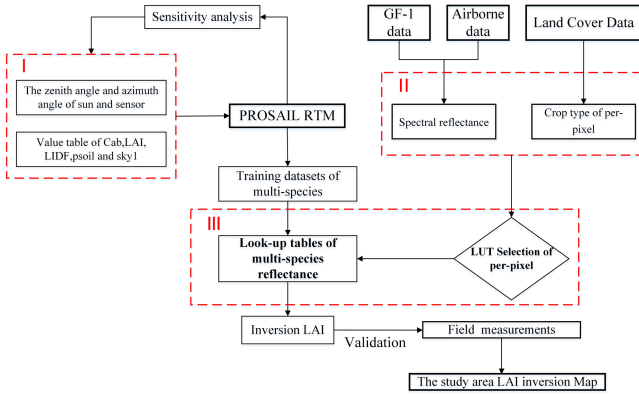


Fig. 3. Framework of the LAI inversion model considering vegetation types.

III. METHODS

A. Framework

The framework of the LAI inversion model considering vegetation types is shown in Fig. 3.

The LAI inversion model considering vegetation types referred to the acquisition of a priori distributions of different vegetation parameters to generate LUTs for specific vegetation types. Afterward, the corresponding LUTs were invoked for the LAI estimation of different vegetation types based on the land cover map and remote sensing data. This algorithm has three key parts as highlighted by the red dotted lines in Fig. 3. The first part is setting the input parameters of PROSAIL according to multispecies vegetation in heterogeneous areas and generating multispecies vegetation LUTs. The second part is determining the band reflectance values and vegetation type of each pixel using the remote sensing data and land cover map and performing LAI estimation on each pixel. The third part is estimating the multispecies LAI in heterogeneous regions while considering vegetation types. According to the vegetation type of each pixel, the corresponding LUT was selected adaptively, and then the LAI of each pixel was estimated based on their band reflectance values. Additionally, sensitivity analysis was performed to evaluate the key input parameters of the PROSAIL model. The performance of the proposed model for estimating multispecies vegetation LAI in heterogeneous regions was then validated, and an LAI inversion map for the study area was generated.

B. PROSAIL Model

The PROSAIL model is a commonly used RTM for the inversion vegetation parameters using physical methods [18]. This method, which is a combination of the PROSPECT [9] and SAIL models [10], was used to generate spectral reflectance for different canopies by setting different input parameters. Table I summarizes the key input parameter distributions of PROSAIL with reference to a priori distributions of the measured data and the related literature [22], [29], [48], [49], [50], [51]. The solar and observation zenith angles were set to 42° and 10° , respectively, based on the flight. According to Table I, the LUTs of multispecies vegetation were generated by the PROSAIL

TABLE I
RANGES AND DISTRIBUTIONS OF PROSAIL INPUT PARAMETERS FOR DIFFERENT VEGETATION TYPES IN THE STUDY AREAS

Input Parameter	Unit	Typical Ranges for vegetation							
		the Nenling study area				the Heihe River Basin study area			
		Winter Wheat	Winter Barley	Rapeseed	Meadow	Shrub	Cultivated Vegetation	Desert Sparse Vegetation	
N	—	1–2.5	1–2.5	1–2.5	1–2.5	1–2.5	1–2.5	1–2.5	
Cab	$\mu\text{g.cm}^{-2}$	40–60	40–65	50–70	0–70	0–70	0–70	0–70	
Car	$\mu\text{g.cm}^{-2}$	10–20	10–25	15–25	0–20	0–20	0–20	0–20	
EWT	cm	0–0.05	0–0.05	0–0.05	0–0.05	0–0.05	0–0.05	0–0.05	
LMA	g.cm^{-2}	0–0.02	0–0.02	0–0.02	0–0.02	0–0.02	0–0.02	0–0.02	
LAI	m^2/m^2	0.5–5	2–7	1.5–6.5	0.3–4	0.3–5	0.5–6	0.1–1	
ALIA	degree	20–70	20–70	20–70	20–70	20–70	20–70	20–70	
Hspot	—	0.01–0.5	0.01–0.5	0.01–0.5	0.01–0.5	0.01–0.5	0.01–0.5	0.01–0.5	
psoil	—	0–1	0–1	0–1	0–1	0–1	0–1	0–1	

TABLE II
RANGES AND DISTRIBUTIONS OF PROSAIL INPUT PARAMETERS FOR ALL VEGETATION TYPES IN THE STUDY AREAS

Input Parameter	Unit	All Vegetation
N	—	1–2.5
Cab	$\mu\text{g.cm}^{-2}$	0–70
Car	$\mu\text{g.cm}^{-2}$	0–20
EWT	cm	0–0.05
LMA	g.cm^{-2}	0–0.02
LAI	m^2/m^2	0.1–7
ALIA	°	20–70
Hspot	—	0.01–0.5
psoil	—	0–1

(N: structure index, Cab: chlorophyll, Car: carotenoid, EWT: equivalent water thickness, LMA: dry matter per area, LAI: leaf area index, ALIA: average leaf inclination angle, Hspot: hot-spot parameter, psoil: soil brightness factor)

model, and then the LAIs of multispecies on the heterogeneous surface were retrieved. Table II shows the uniform model input parameters for all vegetation in the study areas without distinguishing between vegetation types. In the traditional method, all vegetation parameters without considering vegetation types were used to generate LUT to compare its performance with the LAI inversion model considering vegetation types. Afterward, whether the improvement in the LAI inversion accuracy of the heterogeneous surface was due to the advantages of the physical model itself or the consideration of vegetation types was determined.

C. LUT Method

LUT is a large dataset containing canopy spectra corresponding to vegetation parameters. Therefore, the quality of this dataset determines the performance of the LUT. LUT was established by running the PROSAIL model in forward mode to simulate the canopy spectra of different remote sensing images, where the AVIS-3 data contained 146 bands after excluding the effects of water vapor absorption. LUTs were generated separately based on the prior knowledge of each vegetation type (see Table I). To obtain appropriate inversion results and maintain the balance between computational cost and estimation accuracy, the size of different LUTs was set as 100 000 reflectance.

The Laplace distribution (LP) was used as the cost function of LUTs, which is defined as follows:

$$LP = \sum_{i=1}^m |R_{RS,i} - R_{Simulated,i}| \quad (1)$$

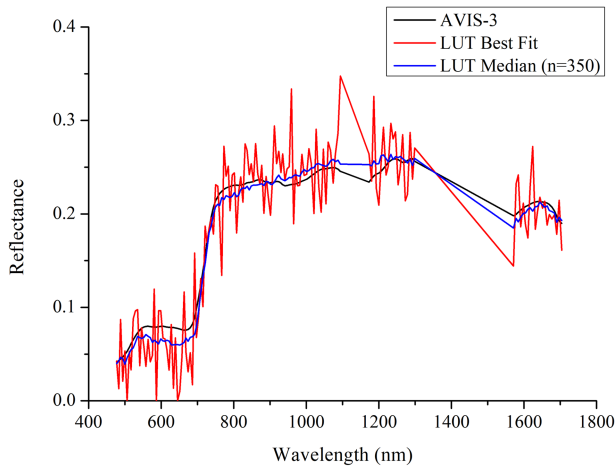


Fig. 4. Comparison of an AVIS-3 reflectance spectrum with the LUT best fit and the LUT median.

where RRS indicates the reflectance of the remote sensing image, R_{simulated} indicates the reflectance simulated by the PROSAIL model, and m indicates the count of spectral bands of the remote sensing image.

To obtain reasonable inverse results, a solution was obtained by the median method of 350 the sorted smallest LP [52]. Fig. 4 compares a randomly chosen reflectance spectrum from the AVIS-3 data with the absolute best fit found by the LUT inversion solution and with the averaged solution (median, $n = 350$). The figure shows how the averaging of multiple solutions affects the fitted reflectance. While the LUT reflectance of the absolute best fit is clearly noisy, the median averaged reflectance adapts to the measured reflectance of AVIS-3.

D. Sensitivity Analysis

For the approach considering vegetation types, the input parameters of PROSAIL need to be set separately according to different vegetation types to generate LUTs. However, the PROSAIL model has multiple input parameters. Therefore, the effect of different input parameters on canopy reflectance must be determined and the key parameters for the differential settings for the proposed approach should be selected. Therefore, a global sensitivity analysis of PROSAIL model was conducted to determine the influence of the input parameters on canopy reflectance. Sensitivity analysis was accomplished by using MATLAB R2015b (MathWorks, Inc.) (GSAT), and the results are shown in Fig. 5 [53], [54].

As shown in Fig. 5, different input parameters have various influences on the canopy spectra. By its definition, the LAI can approximately reflect the canopy structure and leaf area of vegetation [1], [55], [56]. LAI is closely related to photosynthesis and respiration of vegetation, and a change in LAI value will change of vegetation photosynthesis rate, thus affecting the spectral characteristics of vegetation. Hence, it can be observed that LAI affects the whole spectral range. In the VIS band range, the spectrum of vegetation was mainly affected by photosynthesis. The various pigment components contained in the leaf, especially the dominant chlorophyll (Cab), jointly determine the

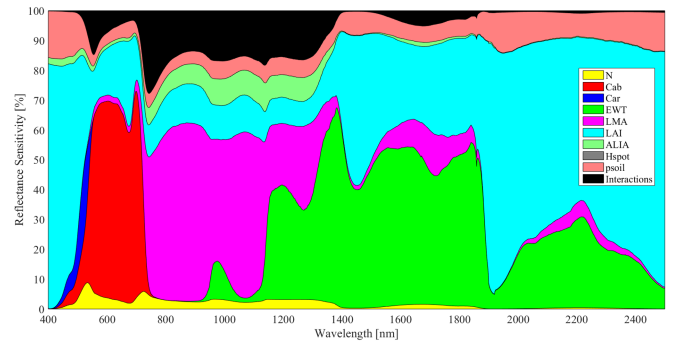


Fig. 5. Text lists the parameters used in the global sensitivity analysis of the PROSAIL model for canopy reflectance, including N (structure index), chlorophyll (Cab), carotenoid (Car), equivalent water thickness (EWT), dry matter per area (LMA), leaf area index (LAI), average leaf inclination angle (ALIA), hot-spot parameter (Hspot), soil brightness factor (psoil), and Interactions (joint global sensitivity for different combinations of parameters).

spectral reflection characteristics of vegetation. Hence, Cab and LAI were the main parameters affecting the canopy reflectance, while the other parameters had a relatively minor effect. For the near infrared (NIR) band range, the effect of leaf on solar radiation changed, and the scattering effect exceeded the absorption effect and became the main behavior. Compared with the leaf pigment content, the cell organization structure of the leaf was the decisive factor affecting its reflection spectral characteristics. The cellulose, lignin, hemicellulose, carbohydrate, starch, and protein contained in leaf are collectively referred to as dry matter per area (LMA). As shown in Fig. 5, the LMA parameter had the greatest effect, followed by LAI. The contribution of equivalent water thickness (EWT) and LAI to canopy reflectance was the greatest in the SWIR band range because EWT determined the spectral reflection characteristics of vegetation. The effect of different input parameters on the canopy reflectance varied widely over the whole wavelength range [57], [58]. The range and distribution of the input parameters were important for canopy reflectance. Meanwhile, the multispecies vegetation varied in leaf optical characteristics, canopy parameters, and soil background. In this case, the ranges and distributions of some input parameters should be set differently depending on vegetation types.

According to the sensitivity analysis, Cab, Car, EWT, and LAI contributed the most to canopy reflectance in the PROSAIL model, hence suggesting that a more accurate range and distribution of these parameters would improve the accuracy of vegetation parameters estimation, which is consistent with the use of a prior information as an effective way to improve the estimation accuracy of canopy variables [28], [59]. In this study, due to the limitations of field measurement, only the different distributions of Cab, Car, and LAI parameters were considered.

IV. RESULTS

A. LAI Estimation for the Neusling Area

The LUTs for multispecies vegetation in the Neusling area were obtained using the PROSAIL model, as shown in Fig. 6. The different colored points, lines, and fitting equations in Fig. 6

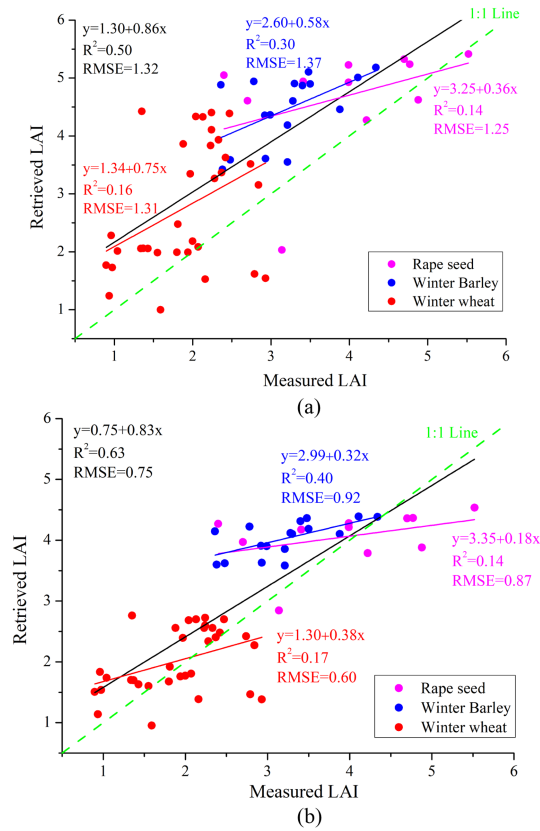


Fig. 6. Scatter plots of field measurement and retrieved LAI for the Neusling area. (a) LAI estimation of all vegetation types using LUT without considering vegetation types. (b) LAI estimation using the approach considering the vegetation types.

represent the LAI estimations for different sampling points. Specifically, magenta represents the fitting result between the measured and estimated values for rapeseed sampling points, blue represents the fitting results for winter barley, red represents the fitting results for winter wheat, and black represents the fitting results for all sampling points.

The correlation between the LAI estimates and measurements was better for the approach considering vegetation types than for the traditional LUT without considering vegetation type, as shown in Fig. 6. The R^2 value increased from 0.50 to 0.63, and the RMSE decreased from 1.32 to 0.75 when using the proposed approach for estimating LAI. R^2 and RMSE had different degrees of improvement and reduction. Given that RMSE is computed as the mean of the square root of the error between the predicted and true values, a smaller RMSE value indicates that the predicted value of the model is closer to the true value. The approach considering vegetation types can efficiently reduce the bias and dispersion of LAI estimation for multispecies in heterogeneous areas. In addition, the LAI values calculated using the approach considering vegetation types were more aggregated in the 1:1 line than those calculated by the LUT method without considering vegetation types. These results demonstrated that the proposed approach is feasible for LAI inversion by considering vegetation types in the heterogeneous regions and can efficiently improve the accuracy of multispecies vegetation LAI estimation.

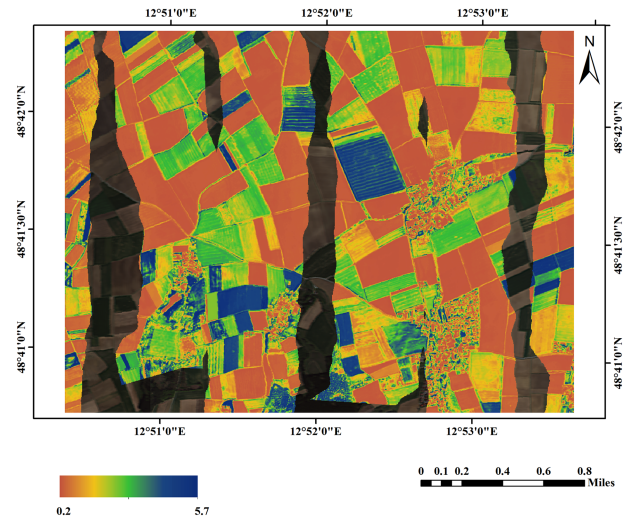


Fig. 7. LAI map of the Neusling area obtained using the approach considering vegetation types (the gaps represent those areas that are not covered by SWIR due to airborne flight striping and where the LAI estimation was not completed due to the lack of SWIR spectral information).

For different crop types, the performance of the approach considering vegetation types varied depending on the crop type. For rapeseed, the R^2 value did not change, but the RMSE dropped from 1.25 to 0.87 when using the approach considering vegetation types. For winter barley, the R^2 increased from 0.30 to 0.40, and the RMSE decreased from 1.37 to 0.92 after using the approach considering vegetation types. The R^2 and RMSE of winter wheat changed from 0.16 to 0.17 and from 1.31 to 0.60, respectively. Therefore, the approach considering vegetation types improved the accuracy of LAI estimation for rapeseed, winter barley, and winter wheat. In particular, the significant reduction of RMSE indicated that this approach can reduce the deviation between the LAI estimates and the measured values.

The LAI map of the Neusling area obtained using the approach considering vegetation types is shown in Fig. 7. The LAI value ranged from 0.2 to 5.7, which highlights the effect of landscape vegetation type on the LAI values. The overall LAI distribution map and the vegetation map [see Fig. 2(a)] showed similar vegetation distribution characteristics and were consistent with the LAI values of the ground measured points. The spectral information of the Neusling area was acquired on April 28 when rapeseed, winter barley, and winter wheat were in their growing season while the other crops were not planted yet. The growth of crops was consistent with the LAI map, and the regions with high LAI values were mainly in rapeseed, winter barley, and winter wheat. In addition, the LAI values in other regions were relatively low, thereby proving the effectiveness of the LAI map obtained by the proposed approach.

B. LAI Estimation for the Heihe Area

The LUTs for the multispecies vegetation in the Heihe area were obtained using the PROSAIL model. The calculated LAIs are shown in Fig. 8, where different colors represent different vegetation types. Specifically, orange represents the fitting result

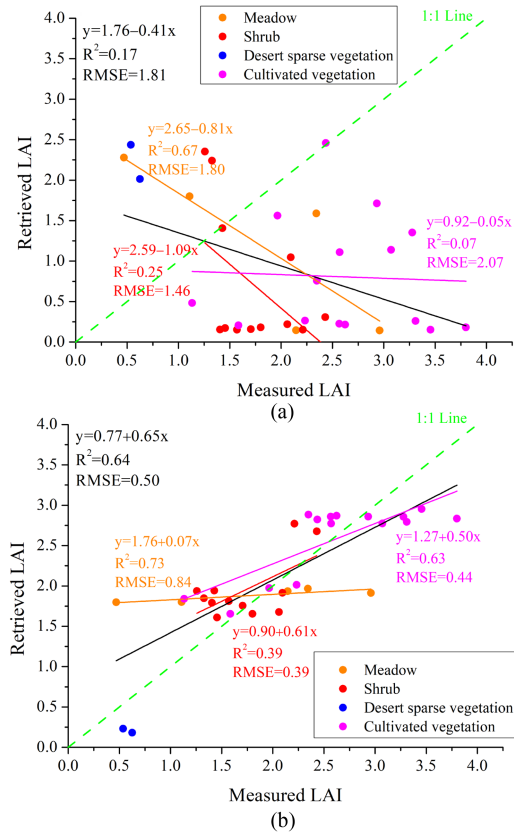


Fig. 8. Scatter plots of the field measured and retrieved LAI for the Heihe area. (a) LAI calculated by using LUT without considering the vegetation types. (b) LAI retrieved by using the approach considering vegetation types.

between the measured and estimated values for meadow, red represents the fitting results for shrub, Magenta represents the fitting results for cultivated vegetation, and Black represents the fitting results for all sampling points.

As shown in Fig. 8(a), a weak correlation was observed between the LAI estimations and measurements, and a negative slope value was obtained for the LUT without considering vegetation types. Therefore, the estimated and measured LAIs exhibited significant differences that do not represent the distribution of LAI in the Heihe area. Meanwhile, a moderate correlation was reported between the LAIs measured and estimated by the approach considering vegetation types. The accuracy of LAI estimation by the proposed approach ($R^2 = 0.64$, $RMSE = 0.50$) was also superior over that of LUT without considering the vegetation types ($R^2 = 0.17$, $RMSE = 1.81$) according to their R^2 values. The LAI values calculated by the approach considering vegetation types were more aggregated in the 1:1 line than those calculated by LUT without considering vegetation types. Therefore, the LAI calculated by the approach considering vegetation types could be applied in the analysis of LAI distribution in the Heihe area. This approach can also extend the application of the PROSAIL model for multispecies LAI estimation in heterogeneous regions.

The LAI estimation performance of the approach considering vegetation types was affected by different vegetation types (see Fig. 8). For meadow, the R^2 value increased from 0.67 to 0.73,

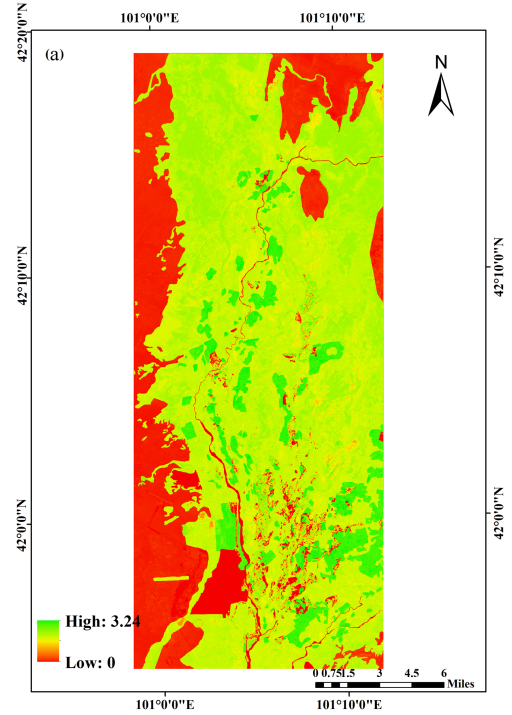


Fig. 9. LAI map of the Heihe area using the approach considering vegetation types.

but the RMSE dropped from 1.80 to 0.84 by using the approach considering vegetation types. For shrub, the R^2 increased from 0.25 to 0.39, but the RMSE decreased from 1.46 to 0.39 after using the same approach. This approach also improved the precision of cultivated vegetation (R^2 from 0.07 to 0.63, RMSE from 2.07 to 0.44) and the accuracy of LAI estimation for meadow, shrub, and cultivated vegetation in the Heihe area. The LAI map of the Heihe area obtained by using the proposed approach is shown in Fig. 9.

Overall, the LAI values in the Heihe study area were low, ranging from 0 to 3.24. The northern and western regions had the lowest LAI values, and the central region had relatively high LAI values. These results may be ascribed to the higher vegetation cover in the central area of Heihe than in its northern and western regions [see Fig. 2(b)]. The northern and western regions are deserts with sparse vegetation and low vegetation cover, whereas the eastern and central regions are mainly covered with shrub interspersed with different vegetation types, such as meadow, cultivated vegetation, and broadleaf forest. The LAI values in the central region were high due to the presence of cultivated vegetation, those in the northern and western desert regions were low, and those in the other regions were moderate due to the presence of meadows and shrubs. Therefore, the LAI distribution and vegetation maps [see Fig. 2(b)] show similar vegetation distribution characteristics, which are consistent with the measured LAI values.

V. DISCUSSION

Given that remote sensing data have a wide observation range and are affected by many factors. Therefore, the influence

of regional heterogeneity on vegetation parameters inversion warrants further study. Darvishzadeh et al. [27] used the LUT method based on the PROSAIL model to retrieve the LAI and leaf Cab of heterogeneous mediterranean grassland. Pasqualotto et al. [60] developed universal canopy water content indices based on the PROSAIL model, which can be used to estimate canopy water content in areas with heterogeneous crop types using remote sensing data. Yao et al. [61] compared and analyzed the LAI inversion performance of different models based on the heterogeneous characteristics of in-row crop structure, and the results showed that the in-line planting model outperformed the other models in the LAI inversion of crops during the early stages of their growth. These studies highlight the potential of the PROSAIL model for estimating the biophysical parameters of heterogeneous areas, which was consistent with the findings of this work.

In heterogeneous regions, the parameters of each vegetation type had different distribution ranges. The proposed approach considered these differences in parameter distributions and provided a priori information on the vegetation parameters, which defined a suitable inversion interval for multispecies LAI. Therefore, the approach considering vegetation types can be applied in the multispecies LAI estimation in heterogeneous regions. As shown in Figs. 6 and 8, this approach was more effective in improving the accuracy of multispecies LAI estimation in the Heihe area than in the Neusling area. Compared with the Heihe area, the Neusling area included different crop types with higher canopy homogeneity. The diverse vegetation types of the Heihe area included desert sparse vegetation, shrubs, meadows, and cultivated vegetation, which exhibited a higher degree of canopy heterogeneity. The PROSAIL model assumed that the vegetation canopy was horizontally homogeneous and extended infinitely, whereas the leaf distribution within the vegetation could be described using a leaf inclination function. This physical assumption did not consider the possible heterogeneity of the vegetation canopy in the horizontal direction, thus limiting its application to heterogeneous scenarios. Therefore, the traditional LUT had low accuracy in the Heihe area ($R^2 = 0.17$), and the method considering vegetation type can better reduce the influence of spatial heterogeneity on the LAI inversion and improve the accuracy of the inversion. Therefore, the approach considering vegetation types extended the application of the PROSAIL model from homogeneous to heterogeneous regions and can significantly improve the accuracy of multispecies LAI estimation in different heterogeneous areas. However, the small number of measurements and parameter types and the presence of measurement errors may cause the priori information to not fully reflect the parameter distributions of different vegetation types, thus affecting the performance of the proposed approach.

Given that the approach considering vegetation types needed to determine the range of biochemical parameters according to the vegetation types, the LAI inversion values may be subjected to errors due to the misclassification of vegetation species. Thus, an accurate vegetation map would improve the classification accuracy and reduce the error of LAI estimation by using the proposed approach. Moreover, the impact of vegetation misclassification on LAI estimation varied across different vegetation

types [62]. A quantitative assessment of the effect of vegetation misclassification on the uncertainty of the LAI product a better estimation of LAI on the heterogeneous surface. Meanwhile, the effect of mixed pixels on the multispecies vegetation LAI estimation needs to be considered. Mixed pixels usually indicate the presence of several vegetation types in a single pixel [63]. Due to surface heterogeneity, a mixture of different features were observed within the image pixel, which affected the accuracy of the LAI product. Nevertheless, remote sensing data with a high spatial resolution were used in the approach considering vegetation types, which can resolve the mixed-pixel problem to some extent. However, mixed pixels are still needed to improve the performance of the approach in the future. The spectral resolution of remote sensing data is among the factors affecting the accuracy of LAI inversion, but increasing the spectral resolution alone did not absolutely improve the accuracy of LAI inversion. Data with higher spectral resolution showed better LAI inversion accuracy and stability if the band was well chosen and the uncertainty in the model parameters was small [64]. Hence, the effect of spectral resolution on LAI estimation should also be considered in the future.

VI. CONCLUSION

To extend the application of the PROSAIL model from homogeneous to heterogeneous vegetation types, an approach considering vegetation types was proposed based on the LUT method and PROSAIL model to estimate multispecies LAI in heterogeneous areas. The experimental results demonstrated that this approach greatly improved the accuracy of multispecies LAI retrieval ($R^2 = 0.63$, $RMSE = 0.75$ / $R^2 = 0.64$, $RMSE = 0.50$) in both study areas with different vegetation distributions, especially for the high canopy heterogeneity. Accurate LAI inversion values can be used to monitor vegetation growth state and accurately estimate crop yield. The proposed approach may extend the application of the PROSAIL model to a heterogeneous surface with complex vegetation. This approach has also proven its feasibility in satellite and airborne images. Future work will focus on applying this approach to a wider range of sensor data and heterogeneous surfaces to improve its applicability and stability. At present, the LAI inversion of canopy coupled leaf optimization model is also being developed by combining leaf scale study with the proposed approach. However, this approach requires further refinement. For instance, while mixed pixels can be alleviated by high-resolution remote sensing images, this problem cannot be avoided. The influence of bare soil in areas with sparse vegetation also needs to be considered. Therefore, in heterogeneous surface LAI inversion, the influence of mixed pixels, bare soil, and other factors on the inversion model should be prevented or reduced.

REFERENCES

- [1] K. Soudani, C. François, G. L. Maire, V. L. Dantec, and E. Dufrière, "Comparative analysis of IKONOS, SPOT, and ETM+ data for leaf area index estimation in temperate coniferous and deciduous forest stands," *Remote Sens. Environ.*, vol. 102, no. 1, pp. 161–175, 2006.
- [2] R. Wells, "Soybean growth-response to plant-density - Relationships among canopy photosynthesis, leaf-area, and light interception," *Crop Sci.*, vol. 31, no. 3, pp. 755–761, May/June 1991.

- [3] M. Campos-Taberner et al., "Multitemporal and multiresolution leaf area index retrieval for operational local rice crop monitoring," *Remote Sens. Environ.*, vol. 187, pp. 102–118, Dec. 15, 2016.
- [4] J. Huang et al., "Improving winter wheat yield estimation by assimilation of the leaf area index from landsat TM and MODIS data into the WOFOST model," *Agricultural Forest Meteorol.*, vol. 204, pp. 106–121, 2015.
- [5] S. Jay, F. Maupas, R. Bendoula, and N. Gorretta, "Retrieving LAI, chlorophyll and nitrogen contents in sugar beet crops from multi-angular optical remote sensing: Comparison of vegetation indices and PROSAIL inversion for field phenotyping," *Field Crops Res.*, vol. 210, pp. 33–46, 2017.
- [6] F. Baret and G. Guyot, "Potentials and limits of vegetation indices for LAI and APAR assessment," *Remote Sens. Environ.*, vol. 35, no. 2/3, pp. 161–173, 1991.
- [7] M. Schlerf and C. Atzberger, "Vegetation structure retrieval in beech and spruce forests using spectrodirectional satellite data," *IEEE J. Sel. Topics Appl. Earth Observ. Remote Sens.*, vol. 5, no. 1, pp. 8–17, Feb. 2012.
- [8] P. P. J. Roosjen, B. Brede, J. M. Suomalainen, H. M. Bartholomeus, L. Kooistra, and J. G. P. W. Clevers, "Improved estimation of leaf area index and leaf chlorophyll content of a potato crop using multi-angle spectral data—Potential of unmanned aerial vehicle imagery," *Int. J. Appl. Earth Observ. Geoinf.*, vol. 66, pp. 14–26, 2018.
- [9] S. Jacquemoud and F. Baret, "Prospect—A Model of leaf optical-properties spectra," *Remote Sens. Environ.*, vol. 34, no. 2, pp. 75–91, Nov. 1990.
- [10] W. Verhoef, "Light-Scattering by leaf layers with application to canopy reflectance modeling—The SAIL model," *Remote Sens. Environ.*, vol. 16, no. 2, pp. 125–141, 1984.
- [11] J.-B. Feret et al., "PROSPECT-4 and 5: Advances in the leaf optical properties model separating photosynthetic pigments," *Remote Sens. Environ.*, vol. 112, no. 6, pp. 3030–3043, 2008.
- [12] J. B. Feret, A. A. Gitelson, S. D. Noble, and S. Jacquemoud, "PROSPECT-D: Towards modeling leaf optical properties through a complete lifecycle," *Remote Sens. Environ.*, vol. 193, pp. 204–215, May 2017.
- [13] J. B. F eret, K. Berger, F. De Boissieu, and Z. Malenovsk y, "PROSPECT-PRO for estimating content of nitrogen-containing leaf proteins and other carbon-based constituents," *Remote Sens. Environ.*, vol. 252, no. 1, 2021, Art. no. 112173.
- [14] S. Jacquemoud, S. L. Ustin, J. Verdebout, G. Schmuck, G. Andreoli, and B. Hosgood, "Estimating leaf biochemistry using the PROSPECT leaf optical properties model," *Remote Sens. Environ.*, vol. 56, no. 3, pp. 194–202, Jun. 1996.
- [15] W. Verhoef, "Earth observation modeling based on layer scattering matrices," *Remote Sens. Environ.*, vol. 17, no. 2, pp. 165–178, 1985.
- [16] G. H. Suits, "The calculation of the directional reflectance of a vegetative canopy," *Remote Sens. Environ.*, vol. 2, no. 1, pp. 117–125, 1971.
- [17] S. Jacquemoud et al., "PROSPECT+SAIL: 15 years of use for land surface characterization," in *Proc. IEEE Int. Conf. Geosci. Remote Sens. Symp.*, 2007, pp. 1992–1995.
- [18] S. Jacquemoud et al., "PROSPECT plus SAIL models: A review of use for vegetation characterization," *Remote Sens. Environ.*, vol. 113, pp. S56–S66, Sep. 2009.
- [19] X. Yao et al., "Estimation of wheat LAI at middle to high levels using unmanned aerial vehicle narrowband multispectral imagery," *Remote Sens.*, vol. 9, no. 12, 2017, Art. no. 1304.
- [20] H. Li et al., "Comparative analysis of GF-1, HJ-1, and landsat-8 data for estimating the leaf area index of winter wheat," *J. Integrative Agriculture*, vol. 16, no. 2, pp. 266–285, 2017.
- [21] L. Wang, T. Dong, G. Zhang, and Z. Niu, "LAI retrieval using PROSAIL model and optimal angle combination of multi-angular data in wheat," *IEEE J. Sel. Topics Appl. Earth Observ. Remote Sens.*, vol. 6, no. 3, pp. 1730–1736, Jun. 2013.
- [22] H. Li, G. Liu, Q. Liu, Z. Chen, and C. Huang, "Retrieval of winter wheat leaf area index from chinese GF-1 satellite data using the PROSAIL model," *Sensors (Basel)*, vol. 18, no. 4, Apr. 6, 2018, Art. no. 1120.
- [23] F. Yang et al., "Comparison of different methods for corn LAI estimation over northeastern China," *Int. J. Appl. Earth Observ. Geoinf.*, vol. 18, pp. 462–471, Aug. 2012.
- [24] B. Koetz, F. Baret, H. Poilve, and J. Hill, "Use of coupled canopy structure dynamic and radiative transfer models to estimate biophysical canopy characteristics," *Remote Sens. Environ.*, vol. 95, no. 1, pp. 115–124, Mar. 15, 2005.
- [25] B. Combal, F. Baret, and M. Weiss, "Improving canopy variables estimation from remote sensing data by exploiting ancillary information. Case study on sugar beet canopies," *Agronomie*, vol. 22, no. 2, pp. 205–215, Mar. 2002.
- [26] S. Jacquemoud, F. Baret, B. Andrieu, F. M. Danson, and K. Jaggard, "Extraction of vegetation biophysical parameters by inversion of the prospect plus sail models on sugar-beet canopy reflectance data—Application To tm and aviris sensors," *Remote Sens. Environ.*, vol. 52, no. 3, pp. 163–172, Jun. 1995.
- [27] R. Darvishzadeh, A. Skidmore, M. Schlerf, and C. Atzberger, "Inversion of a radiative transfer model for estimating vegetation LAI and chlorophyll in a heterogeneous grassland," *Remote Sens. Environ.*, vol. 112, no. 5, pp. 2592–2604, 2008.
- [28] M. Meroni, R. Colombo, and C. Panigada, "Inversion of a radiative transfer model with hyperspectral observations for LAI mapping in poplar plantations," *Remote Sens. Environ.*, vol. 92, no. 2, pp. 195–206, Aug. 15, 2004.
- [29] K. Berger et al., "Evaluation of the PROSAIL model capabilities for future hyperspectral model environments: A review study," *Remote Sens.*, vol. 10, no. 1, 2018, Art. no. 85.
- [30] M. Schlerf and C. Atzberger, "Inversion of a forest reflectance model to estimate structural canopy variables from hyperspectral remote sensing data," *Remote Sens. Environ.*, vol. 100, no. 3, pp. 281–294, Feb. 15, 2006.
- [31] T. Miraglio, K. Adeline, M. Huesca, S. Ustin, and X. Briottet, "Joint use of PROSAIL and DART for fast LUT building: Application to gap fraction and leaf biochemistry estimations over sparse oak stands," *Remote Sens.*, vol. 12, no. 18, 2020, Art. no. 2925.
- [32] C. Bacour, F. Baret, D. B eal, M. Weiss, and K. Pavageau, "Neural network estimation of LAI, fAPAR, fCover and LAI \times Cab, from top of canopy MERIS reflectance data: Principles and validation," *Remote Sens. Environ.*, vol. 105, no. 4, pp. 313–325, 2006.
- [33] S. Jacquemoud, "Inversion of the PROSPECT + SAIL canopy reflectance model from AVIRIS equivalent spectra: Theoretical study," *Remote Sens. Environ.*, vol. 44, no. 2/3, pp. 281–292, 1993.
- [34] C. Bacour, S. Jacquemoud, M. Leroy, O. Hautecoeur, and H. Chauki, "Reliability of the estimation of vegetation characteristics by inversion of three canopy reflectance models on airborne POLDER data," *Agronomie*, vol. 22, no. 6, pp. 555–566, 2002.
- [35] M. Weiss, F. Baret, R. B. Myneni, A. Pragnere, and Y. Knyazikhin, "Investigation of a model inversion technique to estimate canopy biophysical variables from spectral and directional reflectance data," *Agronomie*, vol. 20, no. 1, pp. 3–22, Jan./Feb. 2000.
- [36] R. Darvishzadeh, A. A. Matkan, and A. Dashti Ahangar, "Inversion of a radiative transfer model for estimation of rice canopy chlorophyll content using a lookup-table approach," *IEEE J. Sel. Topics Appl. Earth Observ. Remote Sens.*, vol. 5, no. 4, pp. 1222–1230, Aug. 2012.
- [37] J. Verrelst et al., "Optical remote sensing and the retrieval of terrestrial vegetation bio-geophysical properties—A review," *ISPRS J. Photogrammetry Remote Sens.*, vol. 108, pp. 273–290, 2015.
- [38] F. Baret, J. G. P. W. Clevers, and M. D. Steven, "The robustness of canopy gap fraction estimates from red and near-infrared reflectances: A comparison of approaches," *Remote Sens. Environ.*, vol. 54, no. 2, pp. 141–151, 1995.
- [39] D. Zhang and M. Dietze, "Towards uninterrupted canopy-trait time-series: A Bayesian radiative transfer model inversion using multi-sourced satellite observations," *Remote Sens. Environ.*, vol. 287, 2023, Art. no. 113475.
- [40] J. M. Chen, J. Liu, S. G. Leblanc, R. Lacaze, and J. L. Roujean, "Multi-angular optical remote sensing for assessing vegetation structure and carbon absorption," *Remote Sens. Environ.*, vol. 84, no. 4, pp. 516–525, Apr. 10, 2003.
- [41] R. Darvishzadeh, C. Atzberger, A. Skidmore, and M. Schlerf, "Mapping grassland leaf area index with airborne hyperspectral imagery: A comparison study of statistical approaches and inversion of radiative transfer models," *ISPRS J. Photogrammetry Remote Sens.*, vol. 66, no. 6, pp. 894–906, Nov. 2011.
- [42] S.-B. Duan et al., "Inversion of the PROSAIL model to estimate leaf area index of maize, potato, and sunflower fields from unmanned aerial vehicle hyperspectral data," *Int. J. Appl. Earth Observ. Geoinf.*, vol. 26, pp. 12–20, 2014.
- [43] L. I. Yun-Ling, D. H. Yan, Y. S. Pei, and D. Y. Qin, "Dynamic variation of landscape in heihe river basin," *J. Hehai Univ.: Natural. Sci.*, vol. 33, no. 1, pp. 6–10, 2005.
- [44] Y. Song and Y. Li, HiWATER: Dataset of Leaf Area Index by LAI2000 in the Lower Reaches of the Heihe River Basin, Cold and Arid Regions Science Data Center at Lanzhou, Lanzhou, China, 2015.
- [45] T. B. Hank, M. Locherer, K. Richter, and W. Mauser, "Neusling (Landau a.d. Isar) 2012—A Multitemporal and multisensor agricultural EnMAP preparatory flight campaign (Datasets). V. 1.2. GFZ Data Services," *GFZ Data Services*, 2016, doi: [org/10.5880/enmap.2016.007](https://doi.org/10.5880/enmap.2016.007).

- [46] D. G. Hadjimitsis, C. R. I. Clayton, and V. S. Hope, "An assessment of the effectiveness of atmospheric correction algorithms through the remote sensing of some reservoirs," *Int. J. Remote Sens.*, vol. 25, no. 18, pp. 3651–3674, 2004.
- [47] Y. Zheng and J. Zhou, "Vegetation map 1:100000 of heihe river basin (version 2.0)," *Int. Tibetan Plateau Data Center*, 2015, doi: [org/10.3972/heihe.426.2014.db](https://doi.org/10.3972/heihe.426.2014.db).
- [48] L. Liang, L. Di, and L. Zhang, "Estimation of crop LAI using hyperspectral vegetation indices and a hybrid inversion method," *Remote Sens. Environ.*, vol. 165, pp. 123–134, 2015.
- [49] L. Liang, Z. Qin, and S. Zhao, "Estimating crop chlorophyll content with hyperspectral vegetation indices and the hybrid inversion method," *Int. J. Remote Sens.*, vol. 37, pp. 2923–2949, 2016.
- [50] J. P. Rivera-Caicedo, J. Verrelst, J. Muñoz-Marí, G. Camps-Valls, and J. Moreno, "Hyperspectral dimensionality reduction for biophysical variable statistical retrieval," *ISPRS J. Photogrammetry Remote Sens.*, vol. 132, pp. 88–101, 2017.
- [51] F. Javier Garcia-Haro et al., "Derivation of global vegetation biophysical parameters from EUMETSAT polar system," *ISPRS J. Photogrammetry Remote Sens.*, vol. 139, pp. 57–74, 2018.
- [52] M. Locherer et al., "Retrieval of seasonal leaf area index from simulated EnMAP data through optimized LUT-Based inversion of the PROSAIL model," *Remote Sens.*, vol. 7, no. 8, pp. 10321–10346, 2015.
- [53] F. Cannavó, "Sensitivity analysis for volcanic source modeling quality assessment and model selection," *Comput. Geosci.*, vol. 44, pp. 52–59, 2012.
- [54] P. Bowyer and F. M. Danson, "Sensitivity of spectral reflectance to variation in live fuel moisture content at leaf and canopy level," *Remote Sens. Environ.*, vol. 92, no. 3, pp. 297–308, Aug. 30, 2004.
- [55] J. M. Chen and T. A. Black, "Defining leaf-area index for non-flat leaves," *Plant Cell Environ.*, vol. 15, no. 4, pp. 421–429, 1992.
- [56] J. Delegido, J. Verrelst, C. M. Meza, J. P. Rivera, L. Alonso, and J. Moreno, "A red-edge spectral index for remote sensing estimation of green LAI over agroecosystems," *Eur. J. Agronomy*, vol. 46, pp. 42–52, 2013.
- [57] M. Danner, K. Berger, M. Woche, W. Mauser, and T. Hank, "Fitted PROSAIL parameterization of leaf inclinations, water content and brown pigment content for winter wheat and maize canopies," *Remote Sens.*, vol. 11, no. 10, 2019, Art. no. 1150.
- [58] K. Berger, C. Atzberger, M. Danner, M. Woche, W. Mauser, and T. Hank, "Model-Based optimization of spectral sampling for the retrieval of crop variables with the PROSAIL model," *Remote Sens.*, vol. 10, no. 12, 2018, Art. no. 2063.
- [59] B. Combal et al., "Retrieval of canopy biophysical variables from bidirectional reflectance—Using prior information to solve the ill-posed inverse problem," *Remote Sens. Environ.*, vol. 84, no. 1, pp. 1–15, Jan. 2003.
- [60] N. Pasqualotto, J. Delegido, S. Van Wittenberghe, J. Verrelst, J. P. Rivera, and J. Moreno, "Retrieval of canopy water content of different crop types with two new hyperspectral indices: Water absorption area index and depth water index," *Int. J. Appl. Earth Observ. Geoinf.*, vol. 67, pp. 69–78, 2018.
- [61] Y. J. Yao, Q. H. Liu, Q. Liu, and X. W. Li, "LAI retrieval and uncertainty evaluations for typical row-planted crops at different growth stages," *Remote Sens. Environ.*, vol. 112, no. 1, pp. 94–106, Jan. 15, 2008.
- [62] H. Fang, W. Li, and M. Ranga, "The impact of potential land cover misclassification on MODIS leaf area index (LAI) estimation: A statistical perspective," *Remote Sens.*, vol. 5, no. 2, pp. 830–844, 2013.
- [63] B. Ma et al., "Application of an LAI inversion algorithm based on the unified model of canopy bidirectional reflectance distribution function to the heihe river basin," *J. Geophys. Res.-Atmospheres*, vol. 123, no. 18, pp. 10671–10687, Sep. 27, 2018.
- [64] L. Ke, Q. Zhou, W. Wu, and H. Tang, "Comparison between multispectral and hyperspectral remote sensing for LAI estimation (in Chinese with English abstract)," *Trans. Chin. Soc. Agricultural Eng.*, vol. 32, no. 3, pp. 155–162, 2016.